PLOS | ONE

RESEARCH ARTICLE

Closed-Cell Stent-Assisted Coiling of Intracranial Aneurysms: Evaluation of Changes in Vascular Geometry Using Digital Subtraction Angiography

Ebba Beller[1]*, David Klopp[2], Jens Göttler[1], Johannes Kaesmacher[1], Claus Zimmer[1], Jan S. Kirschke[1], Sascha Prothmann[1]

1 Abteilung für Diagnostische und Interventionelle Neuroradiologie, Klinikum rechts der Isar, Technische Universität München, Munich, Germany, **2** Acandis GmbH & Co. KG, Pforzheim, Germany

* Beller@tum.de

OPEN ACCESS

Citation: Beller E, Klopp D, Göttler J, Kaesmacher J, Zimmer C, Kirschke JS, et al. (2016) Closed-Cell Stent-Assisted Coiling of Intracranial Aneurysms: Evaluation of Changes in Vascular Geometry Using Digital Subtraction Angiography. PLoS ONE 11(4): e0153403. doi:10.1371/journal.pone.0153403

Editor: Utpal Sen, University of Louisville, UNITED STATES

Received: January 18, 2016

Accepted: March 29, 2016

Published: April 13, 2016

Data Availability Statement: All relevant data are within the paper.

Funding: The authors have no support or funding to report.

Competing Interests: Mr. Klopp is employed by Acandis GmbH & Co. KG, Pforzheim, Germany. This does not alter the authors' adherence to PLOS ONE policies on sharing data and materials. The other authors have no conflict of interest.

Abbreviations: SACE, Stent-assisted coil embolization; SWA, sidewall aneurysm; AcomA,

Abstract

Background

Stent-assisted coil embolization (SACE) plays an important role in the treatment of intracranial aneurysms. The purpose of this study was to investigate geometrical changes caused by closed-cell design stents in bifurcation and sidewall aneurysms.

Methods

31 patients with 34 aneurysms underwent SACE with closed-cell design stents. Inflow angle α, determined by aneurysm neck and afferent vessel, and angle between afferent and efferent vessel close to (δ_1), respectively, more remote from the aneurysm neck (δ_2) were graphically determined in 2D angiography projections.

Results

Stent assisted coiling resulted in a significant increase of all three angles from a mean value (±SEM) of α = 119° (±6.5°) pretreatment to 130° (±6.6°) posttreatment ($P \leq .001$), δ_1 = 129° (±6.4°) to 139° (±6.1°), ($P \leq .001$) and δ_2 = 115° (±8.4°) to 126° (±7.5°), ($P \leq .01$). Angular change of δ_1 in AcomA aneurysms was significant greater compared to sidewall aneurysms (26°±4.9° versus 8°± 2.3°, $P \leq .05$). The initial angle of δ_1 and δ_2 revealed a significantly inverse relationship to the angle increase (δ_1: r = -0.41, $P \leq .05$ and δ_2: r = -0.47, $P \leq .01$). Moreover, angle δ_1 was significantly higher in unruptured compared to ruptured aneurysms (135°±7.1° versus 103°±10.8°, $P \leq .05$).

Conclusion

Stent deployment modulates the geometry of the aneurysm-vessel complex, which may lead to favorable hemodynamic changes more similar to unruptured than to ruptured aneurysms. Our findings also suggest that the more acute-angled aneurysm-vessel anatomy, the larger the angular change. Further studies are needed to investigate whether these changes improve the clinical outcome.

anterior communicating artery; BA, basilar artery; MCA, middle cerebral artery; PICA, posterior inferior cerebellar artery; SCA, superior cerebellar artery; ICA, internal carotid artery; d, diameter; SEM, standard error of mean.

Introduction

Stent-assisted coil embolization (SACE) is a well-established endovascular therapy of cerebral aneurysms with wide necks or low dome-to-neck ratios [1–3]. Advantages of SACE over coiling alone are not only mechanical characteristics of the stent, which prevent coil prolapse and allow higher packing density, but also potential hemodynamic effects by diverting the blood flow [4–7]. Besides direct reduction of flow by the stent struts, one of the relevant hemodynamic effects by stent placement seems to be straightening of vessels-aneurysm complex [8]. Especially stents with closed-cell design show this capability of angular remodeling. The closed-cell design makes the stent work as a whole body, immediately transmitting a force used at one end to the other end [9,10]. This leads to effective straightening of a curved vessel in which the stent is implemented [9–11]. Stents with open-cell design show significantly less angular remodeling [11], however, conform better to curved vascular segments by having several independent segments instead [9,10].

Originally, stents have been designed to treat sidewall aneurysms, but it has been shown that stent implementation is also suitable for many bifurcation aneurysms [9]. Advances in SACE have led to a variety of different stent-placement methods, also allowing treatment of a subset of wide-necked aneurysms not amenable to reconstruction with a single-stent due to anatomical conformation. These methods include for example "crossing Y-stent technique", indicating that a second stent is advanced through the first stent interstices and into the contralateral branch vessel [9,12]. Thus a variety of complex aneurysm can be treated with SACE. Previous studies even suggest stent treatment without coiling, already changing hemodynamics sufficiently enough to induce intra-aneurysmal thrombosis [13–15]. Zenteno et al attributed this therapeutic effect to the straightening of the vessel-aneurysm complex induced by balloon inflation during balloon-mounted stent deployment [11,13]. Results of computational flow and ideal aneurysm model analysis also suggest that the straightening of the parent vessel is associated with a favorable outcome [16,17], as it leads to smaller pressure, inflow volume rate and inflow velocity in the aneurysm [16,18]. To investigate the effect of closed-cell stent remodeling in real patients in a clinical setting, we measured structural changes of the vessel–aneurysm complex of bifurcation and sidewall aneurysms treated at our institution.

Materials and Methods

Patient Selection

The study was approved by the ethical committee of the Technische Universität, München. Patient records and information were anonymized and de-identified prior to analysis. We retrospectively identified 50 patients with 57 intracranial aneurysms treated by stent-assisted coiling with closed-cell design stents between June 2008 and July 2015. Patients with no recorded follow-up angiography (n = 13), complication due to dislocation of the proximal part of the stent into the aneurysm (n = 1), postoperative in-stent thrombosis (n = 1) or in-stent occlusion (n = 2) were excluded. No measurement of angular remodeling was possible due to insufficient image quality for the construction of the auxiliary elements in two cases, which were also excluded. The final study population included 31 patients with 34 aneurysms.

Endovascular Treatment

Patients scheduled for elective stent-assisted coiling received oral acetylsalicylic acid (100 mg) and oral clopidogrel (75 mg) for at least 5 days before the procedure. On the day of the procedure platelet function was tested with Multiplate ® Analzyer (Roche Diagnostics, Mannheim, Germany). In case of clopidogrel resistance, clopidogrel was replaced by prasugrel with a loading dose of 60 mg and the procedure was performed the next day. All patients were kept on a

regimen of both acetylsalicylic acid and clopidogrel for 3 months, after which clopidogrel was no longer given

29 aneurysms were treated with single stent-assisted coiling of which 25 were treated with Enterprise stents (Codman & Shurtleff, Inc., Raynham, MA, USA) and of which four aneurysms were treated with Acandis Acclino stents (Acandis, Pforzheim, Germany). One aneurysm was treated with one Enterprise stent and one Solitaire AB stent (Covidien, Irvine, CA, USA), due to distal displacement of the Enterprise stent. From the total amount of 24 bifurcation aneurysms, four were treated in Y-configuration: Two basilar artery (BA) bifurcation aneurysms and one anterior communicating artery (AcomA) aneurysm were treated by placing two Enterprise stents in Y-configuration; One BA bifurcation aneurysm was treated with one Acandis Acclino stent and one Leo stent (Balt, Montmorency, France) in Y-configuration. As Leo stents are made by wire braiding while Enterprise, Solitaire AB and Acandis Acclino stents are laser-cut from nitinol hypotube, the angle formed by the Leo stent was excluded. The Solitaire stent had a diameter of 4 mm, all Acclino and Enterprise stents had a diameter of 4.5 mm.

Vascular Measurements

DSA was performed on a bi-planar Philips Allura Xper FD (Philips Medical Systems B.V., Best, The Netherlands). For assessment of the vessel-aneurysm complex, standard 2D DSA projections angled perpendicular to the longest axis of the aneurysm with the best view of aneurysm sac and neck were analyzed before and after stent-assisted coiling. For graphical measurements of the vascular angles we additionally constructed auxiliary elements with Siemens Solid Edge 2D Drafting as follows (Fig 1). Two circles adjacent to the aneurysm neck were constructed in the efferent and afferent vessel in sidewall aneurysms, respectively, in both efferent vessels in bifurcation aneurysms, with the same diameter as the vessel they were positioned in. An aneurysm neck section line tangential to both circles was drawn. (Fig 1B) A cycle tangential to the aneurysm neck section line and to the afferent vessel was added in bifurcation aneurysms but not in sidewall aneurysms (Fig 1C, lower row). Two more cycles, again with the same diameter of the vessels in which they were positioned in, were added tangentially to each of the previously constructed cycles (Fig 1C). Centerlines were drawn between the centers of the adjacent cycles (Fig 1D). Inflow angle α was determined by the aneurysm neck section line and the centerline of the afferent vessel close to the aneurysm (Fig 1E). The angle close to the aneurysm neck (δ_1) and more remote from the aneurysm neck (δ_2) were determined by centerlines of the efferent and afferent vessel close (δ_1), respectively, located more remotely from the aneurysm neck (δ_2) (Fig 1F and 1G). Two neuroradiologists (EB, SP) evaluated vascular measurements of all aneurysms in consensus reading.

Statistical Analysis

Differences were analyzed using two-tailed Wilcoxon signed rank test or two-tailed Mann Whitney test. Comparisons between three or more groups were analyzed by Kruskal-Wallis (KW) test with post-hoc Dunn's test. Correlation was tested by Pearson's correlation analysis in normally distributed data (prestenting angle) and by Spearman correlation in non-normally distributed data (vessel diameter). Data is presented as means ± SEM. Statistical analysis was performed using GraphPad Prism software (version 5.0a); p-values ≤ 0.05 were considered significant.

Results

Patient and Aneurysm Characteristics

The majority of the patients were women (74.2%) and the median age at stent implementation was 54 years (inter quartile range [IQR]: 44–64 years). Patients presented with subarachnoid

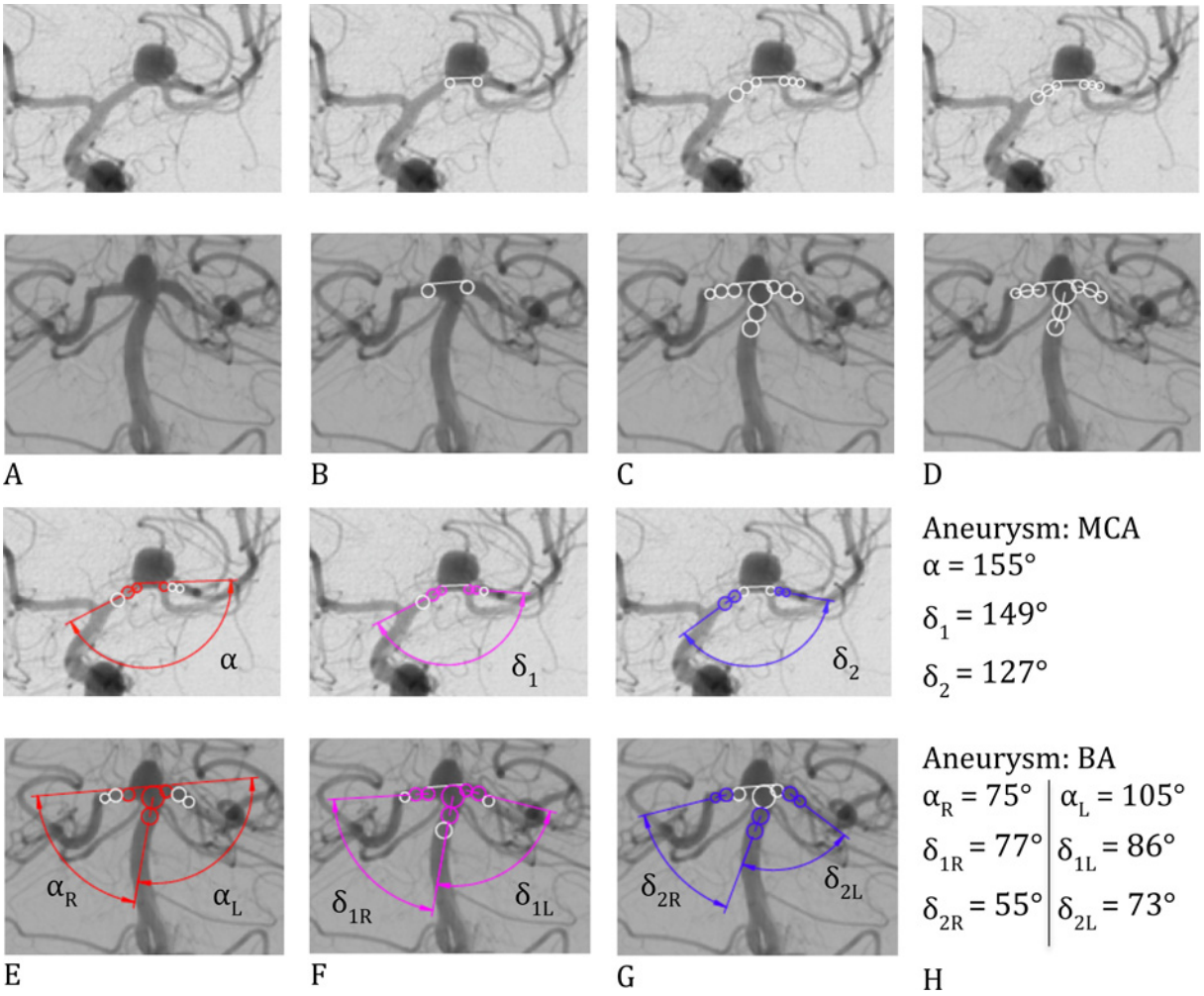

Fig 1. Construction of the auxiliary elements and angular measurements in sidewall and bifurcation aneurysms. Inflow angle α was determined by the aneurysm neck section line and the centerline of the afferent vessel close to the aneurysm. The angle close to the aneurysm neck (δ_1) and more remote from the aneurysm neck (δ_2) were determined by centerlines of the efferent and afferent vessel close (δ_1), respectively, located more remotely from the aneurysm neck (δ_2).

doi:10.1371/journal.pone.0153403.g001

hemorrhage in 11 cases (35%). Bifurcation aneurysms (n = 21) were at the following locations: BA (n = 6), middle cerebral artery (MCA) (n = 5) or AcomA (n = 10). Sidewall aneurysms (SWA) (n = 13) were found at the following locations: BA (n = 2), MCA (n = 1), posterior inferior cerebellar artery (PICA) (n = 1), superior cerebellar artery (SCA) (n = 1) or internal carotid artery (ICA): ophthalmic segment (n = 2) and communicating segment (n = 6). Aneurysm size defined as maximum diameter ranged from 1,5 to 20 mm (median: 7 mm). The size of the aneurysm neck ranged from 1 to 8mm (median: 4mm) with 4 missing values due to absence of calibration. Adjunctive stenting was performed either to treat wide neck aneurysms (n = 18), aneurysm recurrence (n = 8) or due to prolapsed coil (n = 8). No intraprocedural aneurysm rupture occurred during the stent-coiling procedures in any of the patients.

Follow-Up Analysis

For assessment of vessel anatomy, matching 2D projections of the angiograms before and after stent-assisted coiling were analyzed with a median follow-up period of seven months (IQR:

4–11 months). Auxiliary elements for measurement of angle δ_2 could not be constructed in five cases. This was due to the vessel anatomy remote from the aneurysm neck with the course of the vessel orthogonal to the image plane. The diameter of the afferent and efferent vessel was calculated after correction of estimated radiographic magnification factor on digital subtraction angiography. Missing values were due to absence of calibration (no calibration of DSA projections pretreatment = 19, posttreatment = 5), one patient was excluded who developed vasospasm after subarachnoidal bleeding and was treated with nimodipine during follow-up angiography, respectively.

Effective Straightening of the Aneurysm-Vessel Complex after Stent Placement

Changes in all three angles α, δ_1 and δ_2 were detected after stent assisted coiling, suggesting that stent deployment led to effective straightening of the affected vessel. Stent assisted coiling resulted in a highly significant increase of the inflow angle α from a mean value (SEM) of 119° (±6.5°) pretreatment to 130° (±6.6°) posttreatment ($P \leq .001$). Analysis of δ_1 and δ_2, measuring the angle close to the aneurysm neck or more remote from the aneurysm neck respectively, also showed a significant increase of δ_1 from a pretreatment value of 129° (±6.4°) to 139° (±6.1°) posttreatment ($P \leq .001$) and of δ_2 with a pretreatment value of 129° (±6.4°) compared to 139° (±6.1°) posttreatment ($P \leq .01$) (Table 1). The Kruskal-Wallis test with post-hoc Dunn's multiple comparison test showed a significant greater angular change of δ_1 in AcomA aneurysms compared to sidewall aneurysms (26°±4.9° versus 8°± 2.3°, $P \leq .05$), but no significant change of angle α and δ_2. KW test on comparison for angular change between different bifurcation aneurysms (AcomA, MCA and BA) also failed to show significant differences among them (Fig 2).

Relationship between Pretreatment Angle or Vessel Diameter and Angular Change

We hypothesized that the degree of angular remodeling was dependent on the angle of the vessel segment and on the vessel diameter, each before treatment. Analysis of the angular change

Table 1. Angle α, δ_1 and δ_2 before and after stent-assisted coiling.

Location of the Angle	Prestenting Angle			Post-Stent-Coiling Angle		
	α	δ_1	δ_2	α	δ_1	δ_2
Total	119.2±6.5	129.0±6.4	115.0±8.4	130.1±6.6	139.0±6.1	126.2±7.5
	(n = 37)	(n = 37)	(n = 32)	***	***	**
Sidewall	134.8±12.2	145.4±10.8	128.7±14.3	142.0±12.5	153.8±10.5	134.2±14.2
	(n = 13)	(n = 13)	(n = 10)	*	**	ns
Bifurcation	110.8±7.2	111.6±7.0	109.7±10.3	123.6±7.5	131.4±7.2	123.0±8.9
	(n = 24)	(n = 24)	(n = 22)	**	***	*
AcomA	115.8±10.6	124.4±9.6	126.2±14.4	138.5±10.4	150.8±9.9	145.4±14.5
Bifurcation	(n = 11)	(n = 11)	(n = 10)	*	**	**
MCA	141.6±11.6	117.6±16.3	118.8±18.4	148.0±11.9	135.4±16.4	122.2±11.9
Bifurcation	(n = 5)	(n = 5)	(n = 4)	ns	ns	ns
BA	84.6±6.5	90.3±10.4	74.8±12.7	87.8±2.9	102.3±5.6	88.9±7.1
Bifurcation	(n = 8)	(n = 8)	(n = 8)	ns	ns	ns

The p-value applies to the prestenting angle versus the respective post-stent-coiling angle (ns: P>.05, *: $P \leq .05$, **: $P \leq .01$, ***: $P \leq .001$). Prestenting angles have the same number (n) of angle values as post-stent-coiling angles (table shows mean ± SEM).

doi:10.1371/journal.pone.0153403.t001

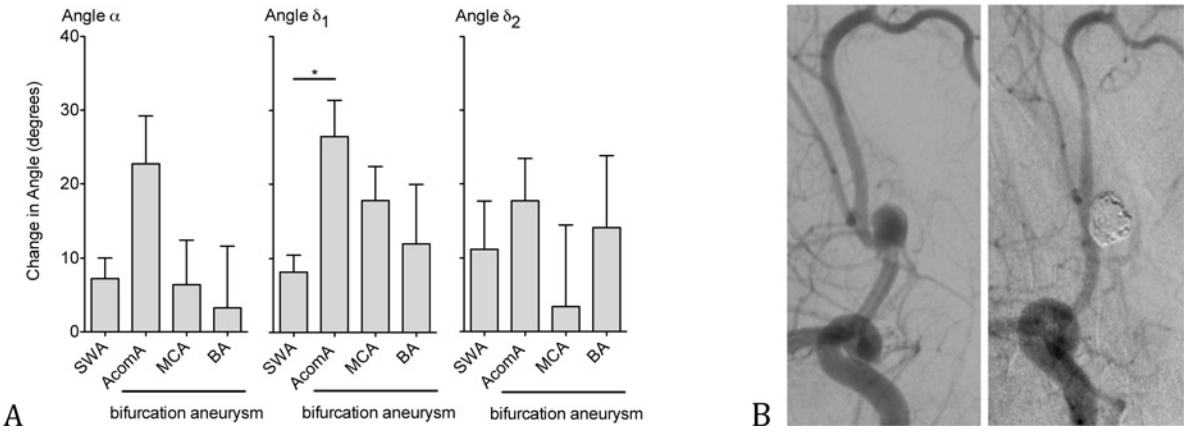

Fig 2. Effective straightening of the aneurysm-vessel complex after stent placement. Angular differences of sidewall and bifurcation aneurysms pre- and posttreatment (A). DSA-Angiography of a 41-year old patient with AcomA aneurysm, showing an effective straightening of the aneurysm-vessel complex 23 months after stent-assisted coiling (B), (graph shows mean ± SEM, *: $P \leq .05$, for n-values see Table 1).

doi:10.1371/journal.pone.0153403.g002

pre- and posttreatment and the pretreatment angle revealed a significantly inverse relationship of angle δ_1 and δ_2 (δ_1: r = -0.41, $P \leq .05$ and δ_2: r = -0.47, $P \leq .01$). There was no significant relationship of the angular change and the prestenting angle of inflow angle α (r = -0.26, P = 0.14) (Fig 3). Analysis of the angular change and the presenting diameter of the proximal (α: r = -0.50, P = 0.06, δ_1: r = -0.05, P = 0.86 and δ_2: r = 0.29, P = 0.33) and distal vessel (α: r = -0.26, P = 0.38, δ_1: r = -0.46, P = 0.11 and δ_2: r = 0.07, P = 0.83) did not show a significant relationship either (n = 18 for α and δ_1, n = 16 for δ_2).

Change in Vessel Diameter of the Afferent and Efferent Vessel After Stent Deployment

The diameter of the proximal (afferent) vessel and the distal (efferent) branch showed a slight yet not significant trend towards an increase from 2.73mm (±0.2mm) pretreatment to 2.90mm (±0.1mm) posttreatment (P = 0.18), and from 2.19mm (±0.2mm) to 2.43mm (±0,1mm), (P = 0.25), respectively (Fig 4).

Angle Formation and Vessel Diameter in Ruptured Aneurysms Compared to Unruptured Aneurysms

Before treatment, angle δ_1 was significantly higher in the unruptured group at 135°±7.1° compared to 103°±10.8° for the ruptured group ($P \leq .05$). Inflow angle α showed greater values in

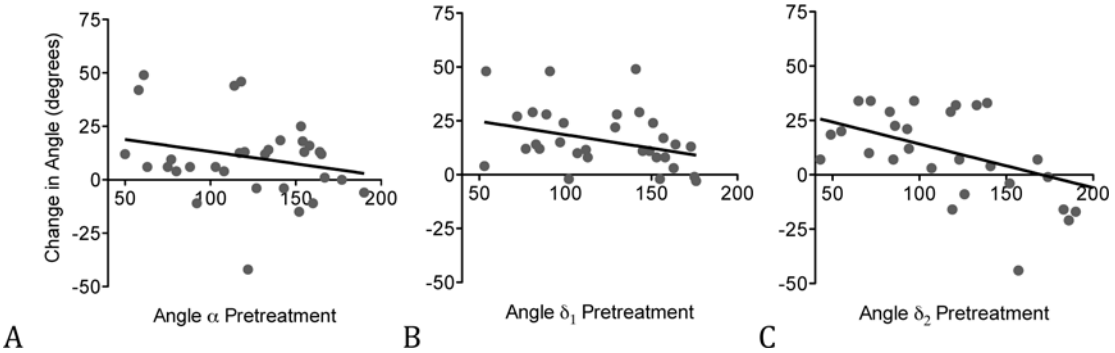

Fig 3. Inverse relationship between the angular change and the pretreatment angle (α, δ_1 and δ_2). α: n = 37, r = -0.26, P = 0.14 (A), δ_1: n = 37, r = -0.41, $P \leq .05$ (B) and δ_2: n = 32, r = -0.47, $P \leq .01$ (C), x axis, angle α, δ_1 or δ_2 before treatment, y axis, angular difference between pre- and posttreatment.

doi:10.1371/journal.pone.0153403.g003

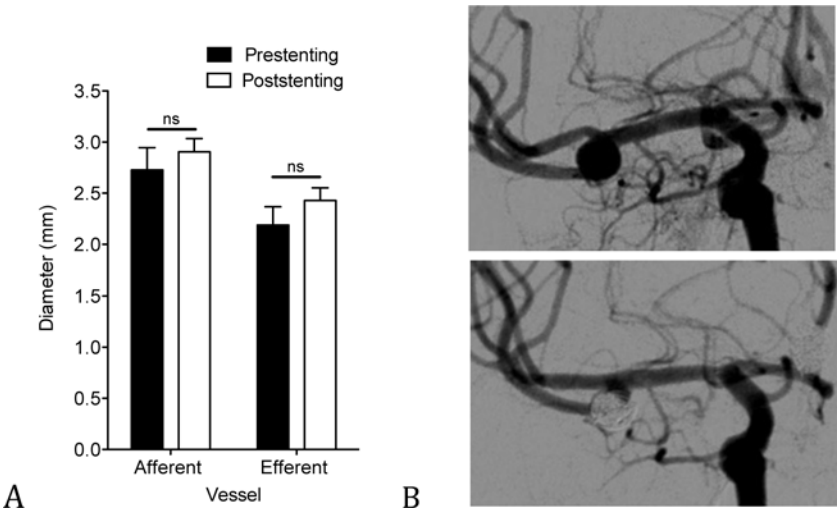

Fig 4. Slight yet not significant increase of the vessel diameter after stenting. Change in vessel diameter of afferent and efferent vessel pre- and posttreatment, n = 18 for the presenting group and n = 30 for the poststenting group (graphs shows mean ± SEM) (A). DSA-angiography of a 43-year old patient with MCA aneurysm showing an increase in diameter especially of the efferent vessel 11 months after SACE (B).

doi:10.1371/journal.pone.0153403.g004

the unruptured subset (138°±8.0°) compared to the ruptured subset (102°±9.7°), almost reaching statistical significance (P = 0.0503). There was no statistically significant difference of angle δ_2 between unruptured aneurysms (119°±9.1°) and ruptured aneurysm (110°±16.3°), (P = 0.28) (Fig 5A). Comparing the diameter of unruptured to ruptured aneurysms, we found a slight trend that did not reach statistical significance towards a greater diameter in the unruptured group compared to the ruptured group. The diameter of the afferent vessel of unruptured aneurysms had a mean value of 2.90mm (±0.28mm) compared to 2.28mm (±0.24mm) of ruptured aneurysms (P = 0.15) and the diameter of the efferent vessel of unruptured aneurysms had a mean value of 2.36mm (±0.22mm) compared to 1.74mm (±0.23mm) of ruptured aneurysms (P = 0.14) (Fig 5B).

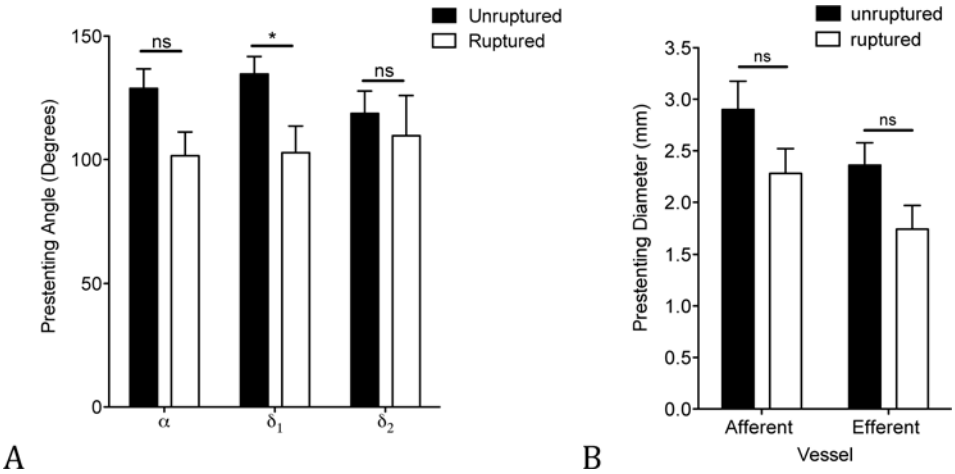

Fig 5. Aneurysm-vessel complex in ruptured aneurysms compared to unruptured aneurysms. Angle of unruptered (α: n = 24, δ_1: n = 24 and δ_2: n = 19) and ruptured aneurysms (n = 13) before treatment (graph shows mean ± SEM, *: P ≤ .05), (A). Vessel size of unruptured (n = 13) and ruptured aneurysms (n = 5) (B).

doi:10.1371/journal.pone.0153403.g005

Discussion

In our study, stent-assisted coil embolization led to effective straightening of the aneurysm-vessel complex and a slight trend towards an increasing vessel diameter. These geometrical changes in SACE are likely to contribute to favorable hemodynamics within the aneurysm.

Hemodynamic factors play an important role in the pathogenesis, progression, and rupture of cerebral aneurysms and are especially sensitive to variations in vessel geometry [16,19–21]. A previous study that used ideal intracranial aneurysm models found a strong dependence of aneurysm hemodynamics on the curvature of the parent artery; the straighter the parent vessel, the smaller the pressure, inflow volume rate and inflow velocity in the aneurysm [16]. Reduction of blood flow into the aneurysm and of the flow velocity magnitude at the neck were found to be related to thrombus formation, supporting a complete occlusion of the aneurysm and a favorable outcome after endovascular treatment [16,17]. Similar results were reported in a study about the hemodynamic effect of changes in key geometrical properties of the aneurysms, using computational fluid dynamics (CFD). After changing a straight parent vessel into a curved one, they observed a drastic change in blood flow dynamics, with an average velocity about ten times higher in the aneurysm sac [18]. Further CFD analysis by Gao et al showed that the bifurcation angle determines the hemodynamic environment of the aneurysm following SACE by changing pressure and wall shear stress in a favorable direction. They could also show that angular remodeling is more significant immediately after Y-stenting and during the first six months of follow-up. Then, a steady state is seen because the potential energy of the stent is mostly released [22,23]. All in all straightening of the aneurysm-vessel complex suggests a favorable hemodynamic change within the aneurysm.

Previous studies mainly focused on vascular remodeling of either bifurcation aneurysms [11,24,25] or sidewall aneurysms only [8,26]. In this study we compared bifurcation to sidewall aneurysms, demonstrating that stent-assisted coiling led to a greater change in the angle of bifurcation aneurysms of the anterior communicating artery compared to sidewall aneurysms. Interestingly sidewall aneurysms, especially of the ACI, compared to bifurcation aneurysm, such as AcomA, have a less acute angle formation before treatment and a greater diameter of the parent vessel. This finding might suggest that the larger the pre-stenting angle and the larger the vessel size, the smaller the angular change of δ_1, δ_2 and also inflow angle α [11]. Other studies on angle remodeling of bifurcation aneurysm after SACE also found this inverse relation between extent of vascular modification and vessel diameter or pretreatment angle, latter corresponding with angle δ_1 of our study [11,24]. In our study we could only show a significant inverse relationship between angular change and presenting angle for angle δ_1 and δ_2 but not between angular change and vessel diameter. The latter could be due to the fact that we had to accept missing values of the vessel diameter (n = 19) because of the absence of calibration.

Previous studies on vascular remodeling effects of SACE have focused on straightening of the parent vessel [20,22,24,25]. In our study we could show that SACE did not only lead to effective straightening but also showed a trend towards an increasing diameter of the parent vessel, suggesting not only a bending [11] but also a radial force exerted by the deployed stent. Studies have shown that specific locations on the cerebral vasculature, e.g. AcomA or distal vessels, have a higher percentage of small ruptured aneurysms compared to other more proximal locations, such as ICA, suggesting a higher rupture risk for aneurysms of vessels with small calibers and lower risks for larger-diameter vessels, independent from aneurysm size [27,28]. In an aneurysm flow dynamics study, Tremmel et al demonstrated that only reducing the diameter of the vessel parent, while keeping all other morphological parameters unchanged, already leads to considerable change in flow patterns to more complex flow structures with multiple associated vortices and an increase of the area exposed to low wall shear stress ($<$0.5 Pa) [29].

Large areas with low wall shear stress on the aneurysm inner wall, which are known to trigger atherosclerotic and inflammatory pathways [21,30,31], as well as complex flow patterns, have been identified to correlate with aneurysm growth [32,33] and rupture [29,30]. Thus, increasing the diameter of the parent vessel and by that decreasing hemodynamic risk factors for aneurysm rupture could be an additional positive effect of SACE.

Comparing ruptured to unruptured aneurysms, ruptured aneurysms seem to have a more acute-angled vessel configuration and a smaller vessel diameter than unruptured aneurysms and by that presumably presenting a high-risk vascular configuration. Previous studies on differences in aneurysm characteristics between ruptured and unruptured aneurysms regarding aneurysm flow angles showed conflicting results [34–37]. Inconsistent results comparing geometric and morphological aneurysm characteristics between patients with ruptured aneurysms and unruptured aneurysms could be due to lack of adjustment for patient specific risk factors for aneurysm rupture or use of different imaging techniques and measurement methodology [37,38]. Moreover, although there is no study about the change of aneurysm-vessel configurations after rupture, it is possible that the event of rupture itself leads to structural remodeling.

The results of our study should be viewed in consideration of its limitations. This was a retrospective study with a relatively small sample size of 31 patients with 34 aneurysms. Further studies with a larger number of patients from multiple centers will be required to verify the findings. This especially applies to the changes in vessel diameter after SACE, as we had to accept missing values due to absence of calibration. Moreover, the sample size of subgroups comparing Enterprise stents with Acandis Acclino stents or Y-configuration with single-stents were too small for statistical analysis. Our hypothesis that increasing the diameter and straightening of the parent vessel contributes to favorable hemodynamics within the aneurysm is supported by previous computational fluid dynamics studies [18,22,29] but has to be corroborated with clinical results and with long-term follow-up angiographic outcomes focusing on recanalization rates.

For graphic analysis of the different angles we used freely available software (Siemens Solid Edge 2D Drafting) and 2D working projections (DSA), which can be easily applied in clinical practice. Although, attention should be paid when performing angle measurements because of large variabilities depending on the viewing angle. As our standard procedure includes the acquisition of a projection perpendicular to the aneurysm, usually by using a 3D DSA-angiography, in order to plan the most effective treatment, we could minimize measurement errors. 3D projections before and after treatment would be preferable for more accurate measurements but were less commonly performed for follow up imaging in our clinical practice.

In conclusion, stent-assisted coil embolization leads to effective straightening of the aneurysm-vessel complex and a trend towards an increase in the diameter of the afferent vessel. These geometrical changes in SACE are likely to contribute to favorable hemodynamics within the aneurysm and are more similar to unruptured than to ruptured aneruysms. Further studies are warranted to investigate whether these changes are associated with a favorable outcome of the patient.

Author Contributions

Conceived and designed the experiments: EB SP DK. Performed the experiments: EB DK SP. Analyzed the data: EB DK SP. Contributed reagents/materials/analysis tools: JSK CZ DK. Wrote the paper: EB SP JG JK JSK SP.

References

1. Biondi A, Janardhan V, Katz JM, Salvaggio K, Riina HA, et al. (2007) Neuroform stent-assisted coil embolization of wide-neck intracranial aneurysms: strategies in stent deployment and midterm follow-up. Neurosurgery 61: 460–468; discussion 468–469. PMID: 17881956

2. Piotin M, Blanc R, Spelle L, Mounayer C, Piantino R, et al. (2010) Stent-assisted coiling of intracranial aneurysms: clinical and angiographic results in 216 consecutive aneurysms. Stroke 41: 110–115. doi: 10.1161/STROKEAHA.109.558114 PMID: 19959540
3. Hetts SW, Turk A, English JD, Dowd CF, Mocco J, et al. (2014) Stent-assisted coiling versus coiling alone in unruptured intracranial aneurysms in the matrix and platinum science trial: safety, efficacy, and mid-term outcomes. AJNR Am J Neuroradiol 35: 698–705. doi: 10.3174/ajnr.A3755 PMID: 24184523
4. Yoo E, Kim DJ, Kim DI, Lee JW, Suh SH (2009) Bailout stent deployment during coil embolization of intracranial aneurysms. AJNR Am J Neuroradiol 30: 1028–1034. doi: 10.3174/ajnr.A1482 PMID: 19193745
5. Balasso A, Bauer JS, Liebig T, Dorn F, Zimmer C, et al. (2014) Evaluation of intra-aneurysmal hemodynamics after flow diverter placement in a patient-specific aneurysm model. Biorheology 51: 341–354. doi: 10.3233/BIR-14019 PMID: 25777299
6. Lopes D, Sani S (2005) Histological postmortem study of an internal carotid artery aneurysm treated with the Neuroform stent. Neurosurgery 56: E416; discussion E416. PMID: 15670395
7. Bendok BR, Parkinson RJ, Hage ZA, Adel JG, Gounis MJ (2007) The effect of vascular reconstruction device-assisted coiling on packing density, effective neck coverage, and angiographic outcome: an in vitro study. Neurosurgery 61: 835–840; discussion 840–831. PMID: 17986946
8. Kono K, Shintani A, Terada T (2014) Hemodynamic effects of stent struts versus straightening of vessels in stent-assisted coil embolization for sidewall cerebral aneurysms. PLoS One 9: e108033. doi: 10.1371/journal.pone.0108033 PMID: 25247794
9. Piotin M, Blanc R (2014) Balloons and stents in the endovascular treatment of cerebral aneurysms: vascular anatomy remodeled. Front Neurol 5: 41. doi: 10.3389/fneur.2014.00041 PMID: 24782817
10. De Bock S, Iannaccone F, De Santis G, De Beule M, Mortier P, et al. (2012) Our capricious vessels: The influence of stent design and vessel geometry on the mechanics of intracranial aneurysm stent deployment. J Biomech 45: 1353–1359. doi: 10.1016/j.jbiomech.2012.03.012 PMID: 22483228
11. Gao B, Baharoglu MI, Cohen AD, Malek AM (2012) Stent-assisted coiling of intracranial bifurcation aneurysms leads to immediate and delayed intracranial vascular angle remodeling. AJNR Am J Neuroradiol 33: 649–654. doi: 10.3174/ajnr.A2841 PMID: 22194381
12. Spiotta AM, Gupta R, Fiorella D, Gonugunta V, Lobo B, et al. (2011) Mid-term results of endovascular coiling of wide-necked aneurysms using double stents in a Y configuration. Neurosurgery 69: 421–429. doi: 10.1227/NEU.0b013e318214abbd PMID: 21389887
13. Zenteno MA, Santos-Franco JA, Freitas-Modenesi JM, Gomez C, Murillo-Bonilla L, et al. (2008) Use of the sole stenting technique for the management of aneurysms in the posterior circulation in a prospective series of 20 patients. J Neurosurg 108: 1104–1118. doi: 10.3171/JNS/2008/108/6/1104 PMID: 18518712
14. Pierot L, Cognard C, Anxionnat R, Ricolfi F, Investigators C (2011) Remodeling technique for endovascular treatment of ruptured intracranial aneurysms had a higher rate of adequate postoperative occlusion than did conventional coil embolization with comparable safety. Radiology 258: 546–553. doi: 10.1148/radiol.10100894 PMID: 21131582
15. Zenteno M, Gomez CR, Santos-Franco J, Vinuela F, Aburto-Murrieta Y, et al. (2010) Ten-year follow-up of giant basilar aneurysm treated by sole stenting technique: a case report. J Med Case Rep 4: 64. doi: 10.1186/1752-1947-4-64 PMID: 20175900
16. Xu J, Wu Z, Yu Y, Lv N, Wang S, et al. (2015) Combined Effects of Flow Diverting Strategies and Parent Artery Curvature on Aneurysmal Hemodynamics: A CFD Study. PLoS One 10: e0138648. doi: 10.1371/journal.pone.0138648 PMID: 26398847
17. Rayz VL, Boussel L, Ge L, Leach JR, Martin AJ, et al. (2010) Flow residence time and regions of intraluminal thrombus deposition in intracranial aneurysms. Ann Biomed Eng 38: 3058–3069. doi: 10.1007/s10439-010-0065-8 PMID: 20499185
18. Seshadhri S, Janiga G, Beuing O, Skalej M, Thevenin D (2011) Impact of stents and flow diverters on hemodynamics in idealized aneurysm models. J Biomech Eng 133: 071005. doi: 10.1115/1.4004410 PMID: 21823744
19. Cebral JR, Castro MA, Appanaboyina S, Putman CM, Millan D, et al. (2005) Efficient pipeline for image-based patient-specific analysis of cerebral aneurysm hemodynamics: technique and sensitivity. IEEE Trans Med Imaging 24: 457–467. PMID: 15822804
20. Huang QH, Wu YF, Xu Y, Hong B, Zhang L, et al. (2011) Vascular geometry change because of endovascular stent placement for anterior communicating artery aneurysms. AJNR Am J Neuroradiol 32: 1721–1725. doi: 10.3174/ajnr.A2597 PMID: 21816920

21. Xiang J, Natarajan SK, Tremmel M, Ma D, Mocco J, et al. (2011) Hemodynamic-morphologic discriminants for intracranial aneurysm rupture. Stroke 42: 144–152. doi: 10.1161/STROKEAHA.110.592923 PMID: 21106956

22. Gao B, Baharoglu MI, Malek AM (2013) Angular remodeling in single stent-assisted coiling displaces and attenuates the flow impingement zone at the neck of intracranial bifurcation aneurysms. Neurosurgery 72: 739–748; discussion 748. doi: 10.1227/NEU.0b013e318286fab3 PMID: 23328687

23. Gao B, Baharoglu MI, Cohen AD, Malek AM (2013) Y-stent coiling of basilar bifurcation aneurysms induces a dynamic angular vascular remodeling with alteration of the apical wall shear stress pattern. Neurosurgery 72: 617–629; discussion 628–619. doi: 10.1227/NEU.0b013e3182846d9f PMID: 23277371

24. Saglam M, Kizilkilic O, Anagnostakou V, Yildiz B, Kocer N, et al. (2015) Geometrical characteristics after Y-stenting of the basilar bifurcation. Diagn Interv Radiol.

25. Cho WS, Kang HS, Kim JE, Kwon OK, Oh CW, et al. (2014) Angle change of the parent arteries after stent-assisted coil embolization of wide-necked intracranial bifurcation aneurysms. Clin Radiol 69: e63–70. doi: 10.1016/j.crad.2013.08.021 PMID: 24286934

26. Zenteno MA, Murillo-Bonilla LM, Guinto G, Gomez CR, Martinez SR, et al. (2005) Sole stenting bypass for the treatment of vertebral artery aneurysms: technical case report. Neurosurgery 57: E208; discussion E208. PMID: 15987592

27. Beck J, Rohde S, Berkefeld J, Seifert V, Raabe A (2006) Size and location of ruptured and unruptured intracranial aneurysms measured by 3-dimensional rotational angiography. Surg Neurol 65: 18–25; discussion 25–17. PMID: 16378842

28. Carter BS, Sheth S, Chang E, Sethl M, Ogilvy CS (2006) Epidemiology of the size distribution of intracranial bifurcation aneurysms: smaller size of distal aneurysms and increasing size of unruptured aneurysms with age. Neurosurgery 58: 217–223; discussion 217–223. PMID: 16462474

29. Tremmel M, Dhar S, Levy EI, Mocco J, Meng H (2009) Influence of intracranial aneurysm-to-parent vessel size ratio on hemodynamics and implication for rupture: results from a virtual experimental study. Neurosurgery 64: 622–630; discussion 630–621. doi: 10.1227/01.NEU.0000341529.11231.69 PMID: 19349824

30. Shojima M, Oshima M, Takagi K, Torii R, Hayakawa M, et al. (2004) Magnitude and role of wall shear stress on cerebral aneurysm: computational fluid dynamic study of 20 middle cerebral artery aneurysms. Stroke 35: 2500–2505. PMID: 15514200

31. Malek AM, Alper SL, Izumo S (1999) Hemodynamic shear stress and its role in atherosclerosis. JAMA 282: 2035–2042. PMID: 10591386

32. Jou LD, Wong G, Dispensa B, Lawton MT, Higashida RT, et al. (2005) Correlation between lumenal geometry changes and hemodynamics in fusiform intracranial aneurysms. AJNR Am J Neuroradiol 26: 2357–2363. PMID: 16219845

33. Boussel L, Rayz V, McCulloch C, Martin A, Acevedo-Bolton G, et al. (2008) Aneurysm growth occurs at region of low wall shear stress: patient-specific correlation of hemodynamics and growth in a longitudinal study. Stroke 39: 2997–3002. doi: 10.1161/STROKEAHA.108.521617 PMID: 18688012

34. Baharoglu MI, Lauric A, Gao BL, Malek AM (2012) Identification of a dichotomy in morphological predictors of rupture status between sidewall- and bifurcation-type intracranial aneurysms. J Neurosurg 116: 871–881. doi: 10.3171/2011.11.JNS11311 PMID: 22242668

35. Lin N, Ho A, Charoenvimolphan N, Frerichs KU, Day AL, et al. (2013) Analysis of morphological parameters to differentiate rupture status in anterior communicating artery aneurysms. PLoS One 8: e79635. doi: 10.1371/journal.pone.0079635 PMID: 24236149

36. de Rooij NK, Velthuis BK, Algra A, Rinkel GJ (2009) Configuration of the circle of Willis, direction of flow, and shape of the aneurysm as risk factors for rupture of intracranial aneurysms. J Neurol 256: 45–50. doi: 10.1007/s00415-009-0028-x PMID: 19221852

37. Backes D, Vergouwen MD, Velthuis BK, van der Schaaf IC, Bor AS, et al. (2014) Difference in aneurysm characteristics between ruptured and unruptured aneurysms in patients with multiple intracranial aneurysms. Stroke 45: 1299–1303. doi: 10.1161/STROKEAHA.113.004421 PMID: 24652309

38. Lauric A, Baharoglu MI, Malek AM (2012) Ruptured status discrimination performance of aspect ratio, height/width, and bottleneck factor is highly dependent on aneurysm sizing methodology. Neurosurgery 71: 38–45. doi: 10.1227/NEU.0b013e3182503bf9 PMID: 22353797